Composition and temperature dependence of the crystal structure of Ni–Mn–Ga alloys

N. Lanska[a)]
Helsinki University of Technology, Laboratory of Biomedical Engineering, P.O. Box 2200, FIN-02015 HUT, Finland and Helsinki University of Technology, Laboratory of Physical Metallurgy and Materials Science, P.O. Box 6200, FIN-02015 HUT, Finland

O. Söderberg, A. Sozinov, and Y. Ge
Helsinki University of Technology, Laboratory of Physical Metallurgy and Materials Science, P.O. Box 6200, FIN-02015 HUT, Finland

K. Ullakko
Helsinki University of Technology, Laboratory of Biomedical Engineering, P.O. Box 2200, FIN-02015 HUT, Finland

V. K. Lindroos
Helsinki University of Technology, Laboratory of Physical Metallurgy and Materials Science, P.O. Box 6200, FIN-02015 HUT, Finland

(Received 2 December 2003; accepted 24 March 2004)

The crystal structure of ferromagnetic near-stoichiometric Ni_2MnGa alloys with different compositions has been studied at ambient temperature. The studied alloys, with five-layered (5M) and seven-layered (7M) martensitic phases, exhibit the martensitic transformation temperature (T_M) up to 353 K. Alloys with these crystal structures are the best candidates for magnetic-field-induced strain applications. The range of the average number of valence electrons per atom (e/a) was determined for phases 5M, 7M, and nonmodulated martensite. Furthermore, a correlation between the martensitic crystal structure, T_M and e/a has been established. The lattice parameters ratio (c/a) as a function of e/a or T_M has been obtained at ambient temperature for all martensitic phases. That the paramagnetic-ferromagnetic transition influences the structural phase transformation in the Ni–Mn–Ga system has been confirmed. © *2004 American Institute of Physics.*
[DOI: 10.1063/1.1748860]

INTRODUCTION

It was recently recognized that ferromagnetic Ni–Mn–Ga alloys with compositions near the stoichiometric Heusler composition Ni_2MnGa are a class of smart materials showing a giant magnetic-field-induced strain (MFIS). The mechanism of MFIS is based on the rearrangement of crystallographic domains (twin variants) in an applied magnetic field, which lowers magnetization energy.[1] This mechanism operates at temperatures below the Curie point (T_C) and martensitic transformation temperature (T_M). The behavior of the material in the magnetic field is determined by such material parameters as magnetocrystalline anisotropy (K_U), saturation magnetization, and mechanical stress necessary for twin variant rearrangement (twinning stress).[2,3]

During the last few years, the Ni–Mn–Ga system has been studied in detail experimentally and theoretically all over the world. It has been found that martensitic and magnetic phase transformation temperatures,[4–9] transformation enthalpy,[5,6] magnetocrystalline anisotropy,[8] and saturation magnetization[8,9] are highly composition dependent. To find the best alloys for practical applications, certain important properties of Ni–Mn–Ga have been mapped with their composition.[9,10] However, the effect of crystal structure on these properties still needs to be clarified in more detail.

The crystal structure of martensite is an important factor that affects both the magnetic anisotropy and mechanical properties of ferromagnetic Ni–Mn–Ga alloys.[11–14] The lattice parameters a and c of the basic martensitic crystal structure (in parent phase coordinates) determine the maximal MFIS value described as $1-c/a$. Almost all of the theoretical maximum values of MFIS have been obtained in five-layered (5M) and seven-layered (7M) martensitic phases in the Ni–Mn–Ga system.[15,16] However, in the nonmodulated martensitic phase (NM) it has not been observed so far, despite the high magnetic anisotropy.[11] The reason for this is the high twinning stress in the NM phase, which was recently confirmed to be approximately 6–18 MPa.[14]

Based on x-ray diffraction data, the unit cell of NM martensite has been determined to be non-modulated tetragonal with ratio $c/a>1$ (in parent cubic phase coordinates).[17] It has been concluded that the crystal structure of 5M and 7M martensitic phases is more complex and that it can be described as the lattice modulated by periodic shuffling along $(110)[1\bar{1}0]_p$ system or with a long-period stacking of $\{110\}_p$ close-packed planes.[17,18] Nevertheless, the basic unit cell of the 5M phase is often approximated to a tetragonal or monoclinic cell with ratio $c/a<1$ (in parent cubic axes), while that of the 7M phase has been determined to be orthorhombic or monoclinic.[17–20]

a)Electronic mail: Nataliya.lanska@HUT.FI

TABLE I. Chemical composition, martensitic transformation temperatures, Curie point, electron concentration, and type of martensitic phase at 298 K in studied alloys.

	Content (at %)			M_S	M_F	A_S	A_F	T_C	e/a	Phase
Alloy	Ni	Mn	Ga	(K)	(K)	(K)	(K)	(K)		
1	50.7	28.4	20.9	334	325	339	345	367	7.685	5M
2	50.7	28.3	21.0	330	323	338	343	363	7.681	5M
3	50.7	27.8	21.5	325	323	331	334	371	7.661	5M
4	50.6	28.5	20.9	333	331	339	341	371	7.682	5M
5	50.0	29.8	20.2	344	340	347	351	370	7.692	5M
6	50.0	28.9	21.1	321	311	320	330	374	7.656	5M
7	49.9	29.9	20.2	344	338	350	354	369	7.690	5M
8	49.7	29.1	21.2	311	309	319	321	372	7.643	5M
9	49.6	29.2	21.2	303	301	309	309	376	7.640	5M
10	49.2	30.6	20.2	328	323	333	337	370	7.668	5M
11	49.1	30.7	20.2	324	321	332	335	370	7.665	5M
12	49.0	30.3	20.7	312	309	318	323	370	7.642	5M
13	48.5	30.3	21.2	302	299	305	308	372	7.607	5M
14	51.0	28.5	20.5	356	350	354	360	365	7.710	7M
15	50.5	29.4	20.1	351	343	348	357	366	7.711	7M
16	49.5	30.3	20.2	341	337	344	348	363	7.677	7M
17	48.8	31.4	19.8	337	333	338	342	368	7.672	7M
18	54.9	23.8	21.3	559	541	568	587	360	7.795	NM
19	54.0	24.7	21.3	497	487	498	510	328	7.768	NM
20	53.9	24.4	21.7	530	524	551	560	336	7.749	NM
21	53.7	26.4	19.9	523	512	538	546	344	7.815	NM
22	53.3	24.6	22.1	465	459	468	476	371	7.715	NM
23	52.9	25.0	22.1	348	344	354	363	356	7.703	NM
24	52.8	25.7	21.5	390	367	377	404	382	7.724	NM
25	52.7	26.0	21.3	434	416	424	446	376	7.729	NM
26	52.4	25.6	22.0	423	414	424	434	375	7.692	NM
27	52.3	27.4	20.3	398	391	403	408	380	7.757	NM
28	51.7	27.7	20.6	383	369	381	394	386	7.726	NM
29	51.5	26.8	21.7	393	374	380	400	377	7.677	NM
30	51.2	27.4	21.4	371	366	371	375	370	7.68	NM
31	51.0	28.7	20.3	379	366	376	385	372	7.721	NM
32	50.5	30.4	19.1	391	376	383	397	378	7.751	NM
33	47.0	33.1	19.9	326	323	329	331	366	7.614	NM

The crystal structure of the Ni–Mn–Ga martensitic phase strongly depends on composition and temperature.[5,18,21,22] The relationship between c/a and the average number of valence electrons per atom (e/a) has been investigated by Tsuchiya *et al.*[21] and Chernenko *et al.*[22] It is pointed out that $e/a=7.7$ corresponds to the crossing of lines T_C versus e/a and T_M versus e/a for Ni–Mn–Ga alloys.[22] This is a critical value, at which the crystal structure of the martensitic phase changes from 5M (with $c/a<1$) to NM (with $c/a>1$). This critical value was estimated by Tsuchiya *et al.*[21] to be $e/a=7.61-7.62$. However, in both publications,[21,22] the data concern mostly the NM phase, while the 7M martensitic phase was not studied and data for the 5M phase were restricted to the alloys with a martensitic phase transformation below ambient temperature.

As mentioned above, only 5M and 7M structures exhibit MFIS. In the present work, the crystal structure of ferromagnetic near-stoichiometric Ni_2MnGa alloys with different compositions in the electronic concentration range from $e/a=7.60$ to 7.82 is investigated. The present research is designed to find the alloy compositions with 5M or 7M structures having the highest possible martensitic transformation temperatures.

EXPERIMENTAL PROCEDURES

The studied Ni–Mn–Ga materials were manufactured at Outokumpu Research Oy and at AdaptaMat Ltd. After ho-

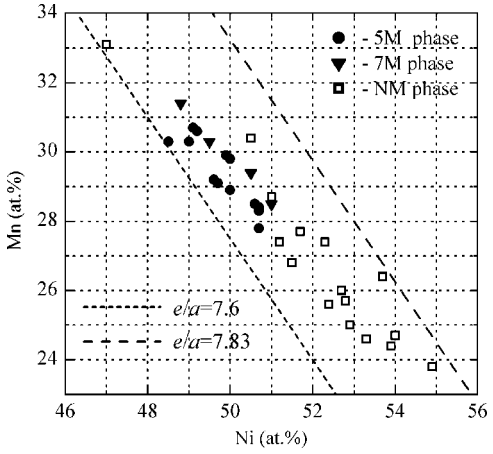

FIG. 1. Ni and Mn content in the studied alloys. The marks correspond to the martensitic crystal structure observed at $T=298$ K. Straight lines indicate compositions with a constant average number of valence electron per atom e/a.

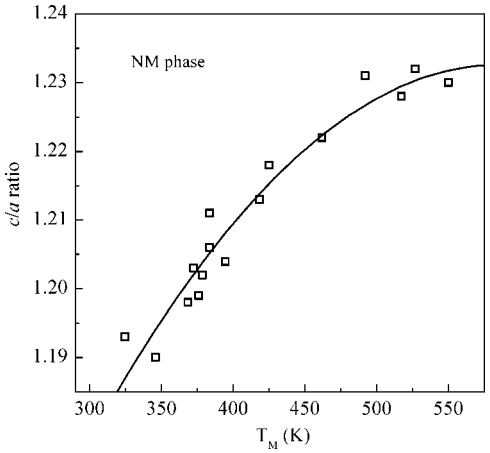

FIG. 2. c/a ratio for the alloys with NM phase at $T=298$ K as a function of the martensitic transformation temperature T_M.

mogenization at 1253 K for 48 h, and aging at 1073 K for 72 h, the ingots were cooled in air to room temperature. The samples with suitable sizes were cut from the ingots with a spark cutting machine. After cutting, the samples were at first wet polished and, finally, electropolished in 25% nitric acid-ethanol solution at a temperature of 273 K for 30 s with 12 V and 0.1 A/mm^2. The chemical compositions were determined by means of a scanning electron microscope equipped with an energy-dispersive spectrometer. Transformation temperatures M_S, M_F, A_S, A_F, and Curie point T_C were measured using low field ac magnetic susceptibility (77–573 K) and a differential scanning calorimeter Linkam 600 (113–873 K). A Philips X'Pert x-ray diffractometer equipped with an Eulerian cradle, Co-tube, and parallel beam optics (x-ray lens and parallel plate collimator with a divergence 0.3°) was used to study the martensitic structure. Texture type and θ–2θ scans were used to find the main Bragg reflections. X'Pert Graphics and Identify software was applied for the analysis of peaks. The lattice parameters of the basic crystal structure were determined in parent phase cubic coordinates, according to the main Bragg reflections. The existence of lattice modulation was confirmed by a linear scan in reciprocal space (Q-scan) between the main peaks in $\langle 110\rangle^*$ direction. Here, the presence of the additional spots, and the number of the intervals into which they divide the distance between the main peaks, indicate lattice modulation and its periodicity.

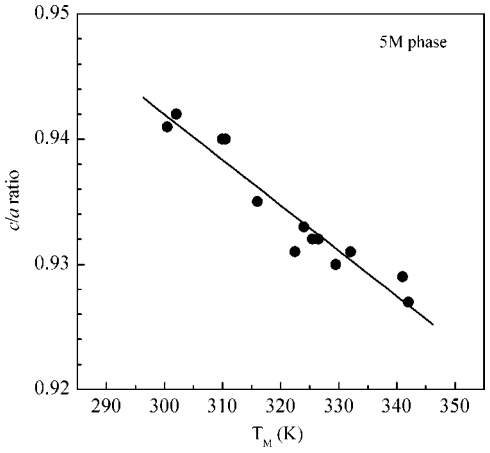

FIG. 3. c/a ratio for the alloys with 5M phase at $T=298$ K as a function of the martensitic transformation temperature T_M.

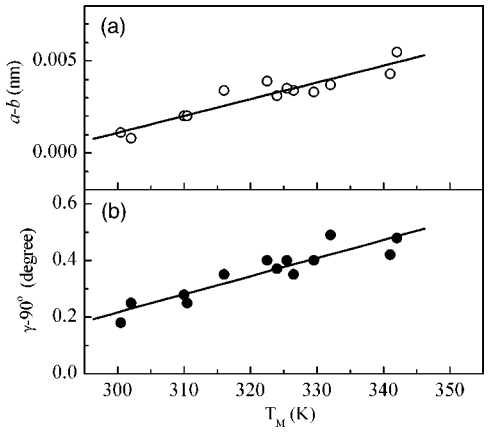

FIG. 4. Monoclinic distortion for the alloys with 5M phase at $T=298$ K as a function of the martensitic transformation temperature T_M. (a) Difference of parameters a and b, (a-b) and (b) deviation of the angle γ from 90°, (γ-90).

RESULTS AND DISCUSSION

Near-stoichiometric Ni_2MnGa alloys with different compositions, exhibiting martensitic transformation temperatures and a Curie temperature higher than 300 K, were chosen for crystal structure study. Consequently, it was possible to carry out x-ray investigation of the ferromagnetic martensitic crystal structures at ambient temperature. The valence electron concentration of the alloys lies in the range from $e/a=7.60$ to 7.82. For calculation of the value for e/a, the valence electrons per atom were 10 for Ni, 7 for Mn, and 3 for Ga.[5] The e/a values for the studied alloys are presented in Table I, together with the chemical composition, the transformation temperatures M_S, M_F, A_S, A_F, Curie temperature T_C, and the martensite type (5M, 7M, and NM). In addition, Fig. 1 shows the Ni and Mn content of the alloys together with the type of martensitic structure observed at room temperature.

In all the alloys with a martensitic transformation temperature T_M above Curie point T_C, the martensite was of the NM type. Here, $T_M=(M_S+M_F)/2$, and M_S and M_F are the start and finish temperatures of the martensitic transformation. Among the alloys with NM martensite at room temperature, there are a few alloys (alloys 23, 24, 28, 30, and 33, see Table I) having $T_M<T_C$. The electron concentration range for the alloys with a NM phase is from $e/a=7.61$ to 7.82, while their T_M is in the wide temperature range of 323–550 K. We confirmed that the unit cell of the NM phase is tetragonal with $c/a>1$. No lattice modulation is observed for this phase. The dependence of c/a on T_M for the alloys with a nonlayered martensitic phase is shown in Fig. 2. The presented data indicate that the lattice tetragonality approaches maximum $c/a\approx 1.23$ at $T_M>550$ K. The tetragonal distortion $(c/a-1)$ decreases with a decreasing T_M.

The 5M phase is found in those alloys with 301 K $\leqslant T_M \leqslant$ 342 K in the electron concentration range from e/a

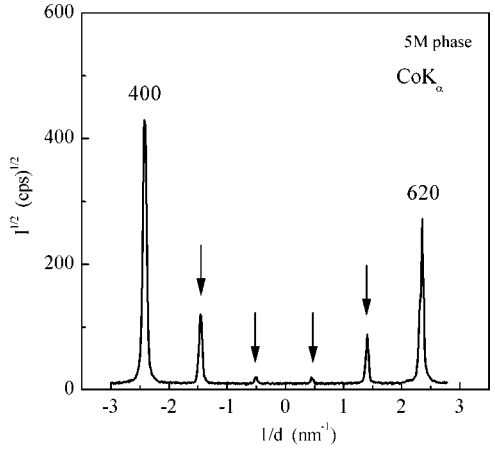

FIG. 5. Scattering intensity distribution along the line between (400) and (620) nodes in reciprocal space for 5M phase (alloy 9). Arrows mark the additional peaks connected with five-layered modulation of the lattice.

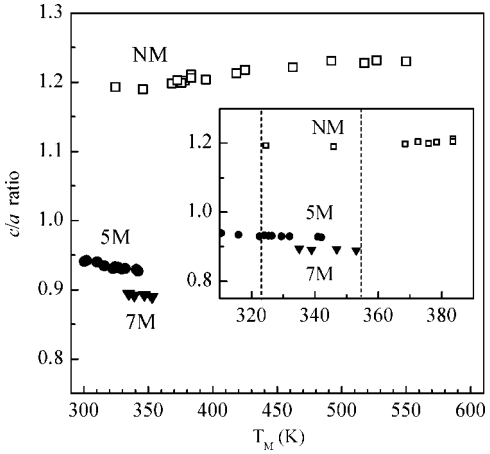

FIG. 7. c/a ratio at $T=298$ K as a function of martensitic transformation temperature (T_M) for the alloys with 5M, 7M, and NM phases. The boundaries in the inset show the temperature range in which all the phases were observed.

$=7.61$ to 7.69. The Curie temperature for such alloys is higher than T_M. The basic unit cell of these alloys is determined as monoclinic with $c/a<1$ and the maximum angle γ between a and b axes 90.50°. The splitting of the main peaks due to monoclinic distortion of the 5M lattice was clearly observed at large 2θ angles. In Fig. 3, c/a ratio of the alloys with a 5M phase is plotted as a function of T_M. The decreasing of T_M leads to the linear increasing of c/a and, consequently, to a decreasing of the maximal theoretical MFIS value described as $1-c/a$. According to Fig. 4, the difference of the lattice parameters a and b, together with the deviation of the angle γ from 90°, becomes smaller with decreasing T_M. Monoclinic distortion of the lattice therefore decreases with a lowering T_M. Five-layered modulation of these alloys is recognized as the four additional spots in the linear scan between (400) and (620) peaks in reciprocal space (see Fig. 5).

Only four of the studied alloys showed a 7M phase at room temperature. Their T_M lies in the narrow temperature range of 335–353 K below T_C, while their e/a is in the range of 7.67–7.71. The basic unit cell for these alloys was found to be monoclinic with $c/a<1$ and angle $\gamma\approx90.5°$. Although the unit cell of both 7M and 5M martensites is monoclinic, the difference between the lattice parameters a and b (0.038–0.040 nm) in 7M martensite is considerably higher than that in 5M martensite. The ratio c/a for 7M martensite is lower than that for 5M martensite. It is approximately of the same value (0.890–0.894) in all studied alloys. The maximal theoretical MFIS value ($1-c/a$) for 7M martensite (~0.11) is higher than for 5M martensite (~0.07). Seven-layered modulation of these alloys has been recognized as the six additional spots in a linear scan between (400) and (620) peaks in reciprocal space (Fig. 6).

The summarized data of c/a versus T_M for all martensitic phases are shown in Fig. 7. There is a specific range, $323\text{ K}<T_M<353\text{ K}$, where alloys with different martensitic phases are simultaneously observed. This same region is present in Fig. 8, in which c/a is shown as a function of e/a for all martensitic phases. Now the multiphase region of e/a is limited with values 7.61 and 7.71. The change from $c/a<1$ to $c/a>1$ takes place within this whole area instead of

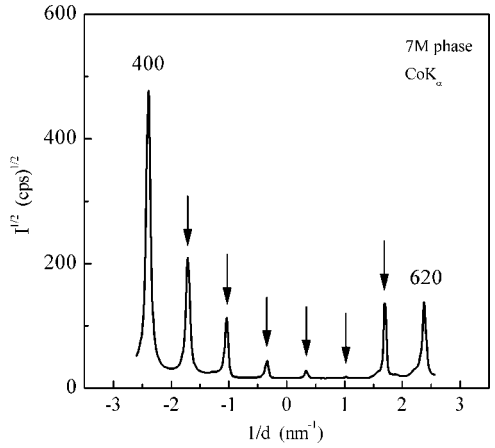

FIG. 6. Scattering intensity distribution along the line between (400) and (620) nodes in reciprocal space for 7M phase (alloy 17). Arrows mark the additional peaks connected with seven-layered modulation of the lattice.

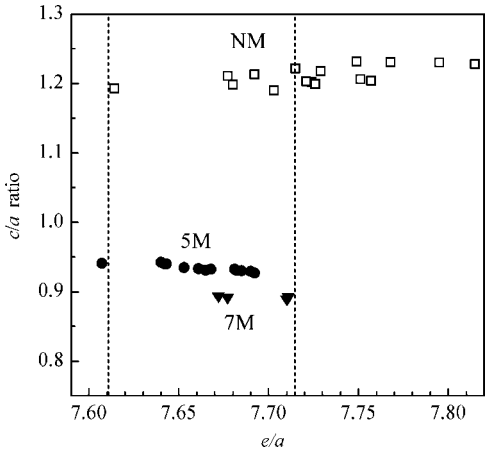

FIG. 8. c/a ratio at $T=298$ K as a function of electron concentration e/a for the alloys with 5M, 7M, and NM phases. The boundaries show the e/a range in which all the phases were observed.

at one sharp boundary. The first limiting value $e/a=7.61$ is in close agreement with the value determined by Tsuchiya *et al.*,[21] while the second $e/a=7.71$ is close to the value determined by Chernenko *et al.*[22] Probably, the closeness of martensitic and ferromagnetic transitions in this range introduces uncertainty to the formation of the structure type resulting from austenite-martensite transformation. In this region, as there is no one-to-one correspondence between crystal structure and a single variable such as T_M or the average number of valence electron per atom e/a, the relation between alloy components should be taken into account. Particularly in the studied set of the alloys, at the same value e/a, increasing the Ni content to above 51 at.% leads to nonlayered, rather than 5M or 7M, structure formation (see Figs. 1 and 8). It should be noticed that the present work is concentrating on the alloys with pure martensitic phases even though the alloys with mixed phases were also observed in the electronic concentration range of 7.61–7.71. Their structure consists of a mixture of 5M and 7M phases or 7M and NM phases, but it was never observed as a combination of 5M and NM phases. According to the present data, for $e/a>7.71$ or $T_M>353$ K, only the NM phase exists, while layered phases (5M and 7M) were observed at lower values of e/a and T_M.

CONCLUSIONS

The correlation between the crystal structure, composition and the martensitic transformation temperature T_M was investigated in near-stoichiometric Ni_2MnGa alloys with T_M above ambient temperatures.

Based on the investigations of the present study the following conclusions can be drawn:

(1) Ni–Mn–Ga ferromagnetic alloys having T_M up to 353 K and a modulated martensitic crystal structure (5M or 7M) were found. They are good candidates for practical applications of magnetic shape memory materials.
(2) The influence of paramagnetic-ferromagnetic phase transformation on the structural phase transformation in the Ni–Mn–Ga system was confirmed. First, if T_M is higher than T_C, only the nonmodulated tetragonal crystal structure (NM) was observed. Second, cubic-5M and cubic-7M martensitic transformations were observed only in the alloys with T_M below T_C.
(3) For the alloys having T_M in the temperature range from 323 to 353 K (10–50 K below the Curie point), there is no one-to-one correspondence between crystal structure and single variables such as T_M or the average number of valence electron per atom e/a. Particularly in the e/a range from 7.61 to 7.72, different crystal structures (5M, 7M, or NM) were observed as a result of martensitic transformation.
(4) The tetragonal distortion of the lattice in the NM phase as well as monoclinic distortion in the 5M phase decreases with decreasing T_M.

ACKNOWLEDGMENTS

The authors would like to acknowledge the funding support given by the National Technology Agency of Finland (Tekes) as well as that from their industrial research partners (Nokia Research Center, Outokumpu Research Oy, Metso Oyj, and AdaptaMat Ltd.) and ONR Project No. N00014-02-1-0462. Furthermore, the help of Dr. Xuwen Liu is gratefully acknowledged.

[1] K. Ullakko, J. K. Huang, C. Kantner, R. C. O'Handley, and V. V. Kokorin, Appl. Phys. Lett. **69**, 1966 (1996).
[2] R. C. O'Handley, J. Appl. Phys. **83**, 3263 (1998).
[3] A. A. Likhachev, A. Sozinov, and K. Ullakko, Proc. SPIE **4333**, 197 (2001).
[4] A. N. Vasil'ev, A. D. Bozhko, V. V. Khovailo, I. E. Dikshtein, V. G. Shavrov, V. D. Buchelnicov, M. Matsumoto, S. Suzuki, T. Takagi, and J. Tani, Phys. Rev. B **59**, 1113 (1999).
[5] V. A. Chernenko, Scr. Mater. **40**, 523 (1999).
[6] S. K. Wu and S. T. Yang, Mater. Lett. **57**, 4291 (2003).
[7] C. Jiang, G. Feng, S. Shengkai, and H. Xu, Mater. Sci. Eng., A **342**, 231 (2003).
[8] F. Albertini, L. Pareti, A. Paoluzi, L. Morelon, P. A. Algarabel, M. R. Ibarra, and L. Righi, Appl. Phys. Lett. **81**, 4032 (2002).
[9] X. Jin, M. Marioni, D. Bono, S. M. Allen, R. C. O'Handley, and T. Y. Hsu, J. Appl. Phys. **91**, 8222 (2002).
[10] I. Takeuchi, O. Famodu, J. C. Read, M. Aronova, K. S. Chang, C. Craciunescu, S. E. Lofland, M. Wuttig, F. C. Wellstood, L. Knauss, and A. Orozco, Nat. Mater. **2**, 180 (2003).
[11] A. Sozinov, A. A. Likhachev, and K. Ullakko, Proc. SPIE **4333**, 189 (2001).
[12] A. Sozinov, A. A. Likhachev, and K. Ullakko, IEEE Trans. Magn. **38**, 2814 (2002).
[13] A. Sozinov, A. A. Likhachev, N. Lanska, O. Söderberg, K. Ullakko, and V. K. Lindroos, Proc. SPIE **5053**, 586 (2003).
[14] A. Sozinov, A. A. Likhachev, N. Lanska, O. Söderberg, K. Koho, K. Ullakko, and V. K. Lindroos, J. Phys. IV (to be published).
[15] J. Murray, M. Marioni, S. M. Allen, R. C. O'Handley, and T. A. Lograsso, Appl. Phys. Lett. **77**, 886 (2000).
[16] A. Sozinov, A. A. Likhachev, N. Lanska, and K. Ullakko, Appl. Phys. Lett. **80**, 1746 (2002).
[17] V. V. Martynov and V. V. Kokorin, J. Phys. III **2**, 739 (1992).
[18] J. Pons, V. A. Chernenko, R. Santamarta, and E. Cesari, Acta Mater. **48**, 3027 (2000).
[19] V. V. Martynov, J. Phys. IV **5**, 91 (1995).
[20] Y. Ge, O. Söderberg, N. Lanska, A. Sozinov, K. Ullakko, and V. K. Lindroos, J. Phys. IV **2**, 921 (2003).
[21] K. Tsuchiya, H. Nakamura, D. Ohtoyo, H. Nakayama, H. Ohtsuka, and M. Umemoto, in *Proceedings of ISAEM 2000: 2nd International Symposium on Designing, Processing, and Properties of Advanced Engineering Materials*, Guilin, China, 20–21 October 2000 (Interscience Enterprises, Ltd., Switzerland, 2001), pp. 409–414.
[22] V. Chernenko, V. L'vov, E. Cesari, J. Pons, R. Portier, and S. Zagorodnyuk, Mater. Trans., JIM **43**, 856 (2002).